A ratiometric optical imaging probe for intracellular pH based on modulation of europium emission

Robert Pal and David Parker*

Received 10th December 2007, Accepted 22nd January 2008
First published as an Advance Article on the web 19th February 2008
DOI: 10.1039/b718993a

A set of three pH-responsive ratiometric Eu(III)complexes has been synthesised incorporating a coordinated azathioxanthone sensitiser and a pH dependent alkylsulfonamide moiety. Emission properties, anion binding affinities, pH response curves and protein binding constants were studied in detail in aqueous media, and solutions containing various concentrations of interfering anions and protein were also examined. The complex, [EuL^3] exhibited some interference from protein and endogenous anions, *e.g.* lactate and hydrogen carbonate, but possessed a protonation constant of 7.2 in human serum solution. A suitable calibration curve was obtained and was used to determine the local pH using a 680/589 nm intensity ratio *vs.* pH plot. Confocal fluorescence microscopy images revealed fast uptake of the complex and a well distributed localisation within the cell; fast egress also occurred. Ribosomal localisation, with a high concentration within the protein-dense nucleoli was observed, in a similar manner to structurally related complexes bearing the same coordinated sensitising moiety. An IC_{50} value of 67 (±20) μM was estimated using an MTT assay. Selected emission band ratio *versus* pH plots allow pH measurement in the range 6 to 8, enabling intracellular pH to be measured by microscopy. A value of 7.4 was estimated for NIH 3T3 cells in the protein rich regions of the nucleolus and ribosomes.

A common strategy to monitor the pH of biochemical events relies on chromogenic pH indicators operating at visible wavelengths. However, in heterogeneous media where indicator concentration or visual observation may be limited, more sensitive indicators and more precise methods are needed to measure pH. This is especially true when monitoring tissue or intracellular pH. To address these problems, a variety of fluorescent probes has been developed to monitor diverse physiological and pathological processes. Acidic environments are known to be associated with poorly vascularised tumours,[1] cystic fibrosis,[2] asthma[3] and several conditions associated with renal dysfunction. For example, intra-tumoural pH was recently reported to range from 6.3 to 7.0,[1,4] and lung airway pH values as low as 5.2 may occur in asthmatics.[3] Acid responsive probes may also find application for cellular imaging of acidic intracellular vesicles, such as endosomes, lysosomes and phagosomes, where pH can range from 4.5 to 6.5.[5] For efficient *in vivo* imaging, dyes that absorb and emit in the visible or NIR region are promising due to the increased optical transparency and lower tissue autofluorescence in this régime.[6]

A wide variety of optical probes for studying proton concentrations[7–10] in biological environments has been reported. Two main optical methods may be considered in defining probes for imaging local pH: nano-crystals,[8,10] *e.g.* those based on surface-modified CdSe crystals, relying on fluorescence energy transfer (FRET) as the signal transduction mechanism, or the large class of low MW organic fluorophores.[11,12] The application of these sensors is limited by one or more of the following properties: low water solubility leading to the need for a co-solvent, a pH-dependent quantum yield, sub-optimal pK_a value, a small Stokes' shift and low sensitivity because their photoactivity may lie in the spectral window where endogenous chromophores may either absorb or fluoresce. Most importantly, they usually do not possess the property of ratiometric analysis,[13] as the pH is often signalled by emission intensity changes in a single broad band. Hence, their use may be highly concentration dependent, compromising accuracy.

In designing a practicable luminescent probe of pH that is suitable for usage inside living cells and may be examined by spectroscopy and microscopy, several exacting constraints must be addressed. The complex must be cell-permeable, kinetically stable and non-toxic; it should be excited at a wavelength above 340 nm, preferably corresponding to a common laser or LED emission (*e.g.* 355, 365 or 405 nm); it should signal changes in local pH reversibly by a modulation of the intensity of at least two emission bands, thereby allowing a ratiometric measurement; it should possess a large Stokes shift to minimise autofluorescence and preferably possess a long excited state lifetime, permitting the use of time-resolved methods.

Several different approaches to luminescent pH probes are being devised and emissive lanthanide complexes intrinsically are particularly well suited for this purpose. Various examples of responsive europium and terbium complexes have been reported over the past few years,[14,15] that satisfy some of these criteria. For example, a reversible pH-dependent intramolecular sulfonamide ligation mode (Scheme 1) has been engineered into macrocyclic Eu complexes.[16] These original systems lacked direct usage, as the sensitising moiety was integrated into the sulfonamide group. Therefore, the distance of the sensitiser from the europium ion was also pH-dependent and overall emission intensities fell on acidification, in parallel with changes of emission spectral form, precluding accurate ratiometric analysis. Such a problem can be

Department of Chemistry, Durham University, South Road, Durham, DH1 3LE, UK. E-mail: david.parker@durham.ac.uk

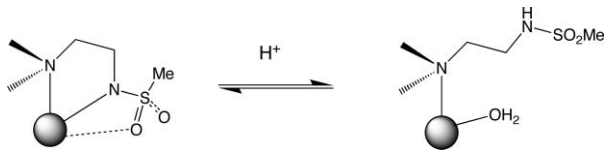

Scheme 1

obviated by integrating the sensitiser into the ligand structure in a manner that is independent of the sulfonamide moiety.

The emission spectrum of europium(III) complexes is a particularly sensitive function of the local coordination environment provided by the ligand. Both the local symmetry around the metal and the charge and polarisability of the donor atoms determine the relative intensity of the emission bands from the $^5D_0$ excited state.[17a,17b] This is most apparent in changes in the form and intensity of the hypersensitive $\Delta J = 2$ (610–630 nm) and $\Delta J = 4$ (680–710 nm) bands. Emission bands within these electric-dipole allowed transitions are particularly sensitive to the polarisability of the axial donor ligand[17] and an intense 680 nm transition in the $\Delta J = 4$ manifold has been observed for several complexes with axial N ligation.[18,19] For example, the switch from the binding of the sulfonamide N to europium(III) to (Scheme 1) ligation by water or an intramolecular carboxylate group, may be signalled by a diminution in the relative intensity of the 680 nm band.[16]

Herein, we report details of the synthesis and characterisation of a set of three putative pH probes and the selection and application of the best system for pH measurement within cells. A preliminary account of aspects of this work has appeared.[17c]

Ligand and complex synthesis

A set of three macrocyclic europium complexes, [EuL^1–L^3], was designed incorporating an N-linked methylsulfonamide moiety, as well as a sensitising group that remains bound to the metal centre as the pH is varied. The ligand switches coordination number from 8 in basic media to 7 in acidic media, following protonation of the sulfonamide N. Such a change is then signalled by modulation of the spectral form of the emission from the Eu ion, allowing pH to be monitored by examining the intensity ratio of pairs of emission bands.

The chromophore selected was an azathiaxanthone, as it allows long wavelength excitation of Eu(III) in the range 355 to 405 nm and can be synthesised quickly and efficiently.[19,20] Reaction of 2-bromomethyl-1-azathiaxanthone with the appropriate 1,7-disubstituted ester in dry MeCN in the presence of $NaHCO_3$ at 70 °C led to formation of the mono-alkylated adduct. This was separated from any dialkylated material by column chromatography. Subsequent reaction with *N*-mesylaziridine, or its acyclic mesylate precursor, (MeCN, K_2CO_3) afforded the desired ligand. Acid or base-catalysed hydrolysis of the ester groups (TFA–CH_2Cl_2 for removal of ^{t}Bu groups; KOH–H_2O for hydrolysis of Me esters) gave the ligands L^1–L^3. Complexation of each of these ligands with a suitable europium salt, *e.g.* $Eu(OAc)_3$ in aqueous methanol afforded the desired 1 : 1 lanthanide(III) complex. The acetate or chloride anion complexes (obtained, if necessary, by anion exchange chromatography) were used to enhance the water solubility of the complex. The homogeneity of each complex was established by reverse-phase HPLC, and each gave a high resolution mass spectrum with the appropriate isotope ratio and calculated mass. Proton NMR spectra of each complex were found to be exchange broadened in aqueous solvents, over the observed 200–700 MHz frequency régime, at ambient temperature. Irrespective of the nature of the ligand, a bathochromic (red) shift was observed following Eu coordination, both in absorption (380 nm) and emission (440 nm). A small increase was also observed in the molar extinction coefficient of the azathioxanthone moiety, *e.g.* from 4070 cm^{-1} to 5130 cm^{-1} (in H_2O for [EuL^3]), whilst a 200 cm^{-1} increase in the sensitiser triplet energy (22 800 cm^{-1} for [GdL^1]) was measured (77 K, EPA glass), following ligation of the pyridine to the europium centre.

Emission spectra for the Eu(III) complexes were examined as a function of pH (0.1 M NaCl, 298 K) in aqueous media. For both [EuL^1] and [EuL^3], substantial and reversible changes were observed in the splitting of the $\Delta J = 1$ transition and the form of the $\Delta J = 2$ and $\Delta J = 4$ manifolds; new bands appeared at 627 nm and 680 nm as the pH was raised from 5 to 8. For example, for [EuL^3] a plot of the change in the emission intensity ratio (680/587 nm) *versus* pH (Fig. 1) revealed an 80% change in this ratio (pH 4.5 to 8). Apparent protonation constants of 6.15 (±0.05) [EuL^3] and 6.1 (±0.1) for [EuL^1] were estimated, fitting the variation of this ratio with pH by iterative non-linear least squares

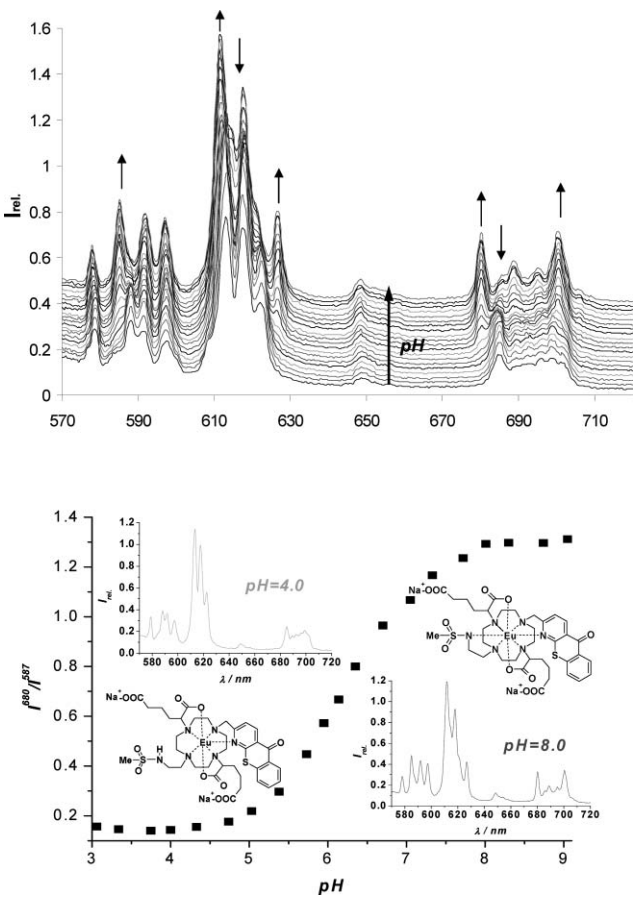

Fig. 1 (*upper*) pH dependence of the metal-based emission spectrum of [EuL^3], (λ_{exc} 380 nm, 0.1 M NaCl, 298 K); (*lower*) intensity ratio *vs.* pH plot with a protonation constant, pK_a = 6.15 (±0.05), highlighting the dominant Eu(III) species at the limiting ratios and their Eu(III) emission spectra.

fitting. Very similar values were obtained (±5%) by examining changes in the intensity ratio of other pairs of emission bands, *e.g.* 618/627 or 612/618 nm.

With [EuL^2], each of these intensity ratios was more or less invariant over the pH range 4.5 to 7. Only above pH 7.5 was the appearance of the 627 and 680 nm emission bands more evident (Fig. 2). By fitting the changes in emission intensity ratio with pH to two successive protonation constants, values of 4.5 (±0.1) and 7.6 (±0.1) could be estimated. These relate to protonation of the Eu bound side-chain carboxylate and sulfonamide N, respectively. Such behaviour accords with earlier observations[16] with analogues of [EuL^2], in which intramolecular carboxylate ligation, leading to formation of a seven-ring N–O chelate, competes with 5-ring sulfonamide chelation. The binding of the carboxylate group is suppressed with [EuL^3], due to unfavourable 8-ring chelate formation.

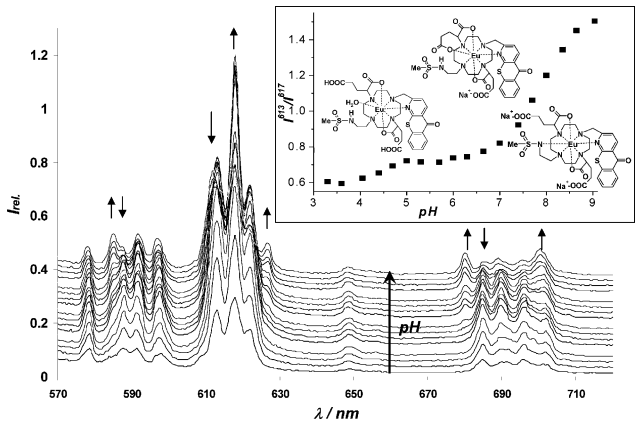

Fig. 2 Variation of the europium emission with pH for [EuL^2] (λ_{exc} 380 nm, 0.1 M NaCl, 298 K, [complex] = 20 μM) showing (insert) an emission intensity ratio *vs.* pH plot, with key species highlighted.

Photophysical data (radiative rate constants and quantum yields) were measured for each complex at pH 4.5 and 8; for [EuL^2], the values in acidic media were recorded at pH 3 and 5.5 (Table 1). Changes in complex hydration state, q, were assessed by measuring the radiative rate constants for excited state depopulation in H_2O and D_2O using an established relationship to deduce the number of water molecules bound to Eu.[21] In each case at pH 8, a q value of zero was obtained, with partial hydration only in more acidic media (q = 0.6 at pH 4.5 for [EuL^1] and [EuL^2]). With [EuL^3], the hydration state apparently remained near zero over the entire pH range, with a slightly higher overall emission quantum yield (*ca.* 6%). The lower hydration of this complex throughout the pH range, must reflect the greater steric demand imposed by L^3, about the Eu centre. Confirmation of this behaviour was obtained by examining the pH dependence of [GdL^3]: the measured relaxivity was 3.1 mM^{-1} s^{-1} (±0.2) over the pH range 3 to 5.5 and reduced to 1.9 mM^{-1} s^{-1} at pH 8.5. From the variation of relaxivity with pH, an apparent protonation constant of 6.2 (±0.15) was estimated, agreeing well with the value obtained from luminescence emission experiments. These low relaxivity values are consistent with the behaviour of a q= 0 complex,[22] with the changes reflecting modulation of the extent of the second sphere of hydration.

Table 1 Radiative rate constants, k^b (ms^{-1} ± 10%) for depopulation of the Eu $^5D_0$ excited state, metal hydration states, q^a (± 0.2) and overall absolute emission quantum yield (± 20%) for Eu complexes (λ_{exc} 384 nm, 298 K)

Complex	pH	k_{H2O}	k_{D2O}	q^{Eu}	$\phi_{em}{}^c$ (%)
EuL^1	4.5	2.08	1.32	0.62	0.9
	8.0	2.43	2.10	0.10	1.0
EuL^2	3.0	1.70	0.92	0.65	1.7
	5.5	1.41	1.00	0.19	2.0
	8.0	2.13	1.87	0.01	1.8
EuL^3	4.5	1.36	1.21	0	6.1
	8.0	2.38[d]	2.12	0.01	5.4[e]

[a] q Values were estimated according to reference 21 and assume fast NH/ND exchange for unbound sulfonamides. [b] Values represent the mean of three separate measurements. [c] The error on quantum yield values is estimated to be ±20%. [d] Reduces to 1.61 ms^{-1} in human serum solution at pH 7.4. [e] Increases to 14% in human serum solution.

Behaviour of complexes in the presence of anions

In order to judge whether the europium complex was suitable for biological applications, the emission behaviour was examined in the presence of common bioactive anions. Preliminary studies involved pH titration of a given Eu(III) complex, in a 'simulated extracellular' ionic background (0.9 mM hydrogen phosphate; 0.13 mM citrate; 2.3 mM lactate; 30 mM bicarbonate and 0.1 M chloride, each as sodium salts). Each complex exhibited some anion sensitivity in the observed pH régime (3 to 9). In order to understand the complexity of these titrations and to determine the nature of the predominant [EuL^n(anion)$_x$] ternary species in solution, pH titrations were also undertaken using individual anion solutions. To avoid a significant change in the ionic strength of the sample, a common background of 0.1 M NaCl was used. If a particular anion revealed an affinity towards the given complex, titrations were undertaken increasing the anion concentration up to its limiting extracellular concentration value, maintaining a constant pH. Such detailed studies allowed the limiting spectral form of a given ternary anion adduct to be established. The characteristic spectral features serve to act as a fingerprint for this species, allowing the distinction to be made between different adducts in solutions containing mixtures of anions.

As an example of this approach, the behaviour of [EuL^3] may be considered first. The pH dependence of the Eu spectral profile (Fig. 3), in the simulated extracellular fluid solution was studied. Pronounced changes in the form and intensity of bands within the ΔJ = 2 and ΔJ = 4 manifolds were observed. For example, the 680 nm band reports on intramolecular sulfonamide N ligation over the range 5 to 7,[16a] whilst the relative intensity of the 613/615/617 bands may be associated with competitive intermolecular carbonate ligation.[16b]

In studies with single added anions, no significant changes over the pH range 3 to 9 were observed in the Eu emission profile with either added hydrogen phosphate or added citrate, up to 2 mM concentrations. Moreover, addition of up to 1 mM concentrations of ascorbate and urate neither perturbed the intensity of the emission spectrum nor changed the measured radiative lifetime, consistent with an absence of static and dynamic quenching from these low MW reductants.[19a] In contrast, spectral titrations (0.1 M NaCl, 298 K 5 μM [complex]) with either hydrogen carbonate or lactate revealed distinctive emission intensity changes. In

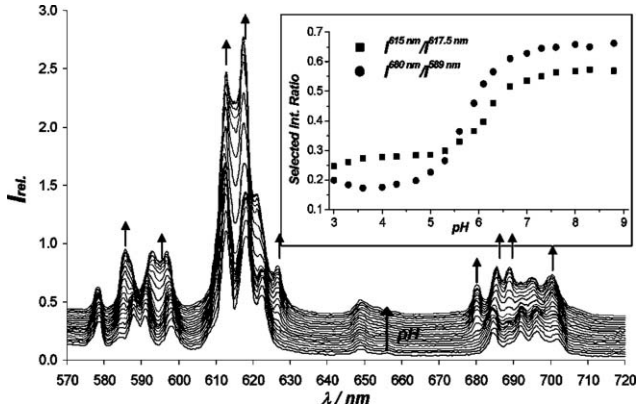

Fig. 3 Variation of Eu emission in [EuL^3] with pH, using a simulated extracellular anion fluid as the background medium ([complex] = 20 μM, 298 K, λ_{ex} = 380 nm, I = 0.1 M NaCl). (insert): intensity ratio (squares; 615/617.5 nm and circles: 680/598 nm) *vs.* pH plots, indicating the presence of differing [EuL^3(anion)] species at the limiting ratios.

these cases, each anion is able to bind to the Eu centre, and apparent affinity constants were able to be measured. A log K value of 2.75 was estimated for lactate at pH 5.5, and 4.09 for hydrogen carbonate at pH 7.4 (Table 2). Supporting evidence for a 1 : 1 stoichiometry of binding came from electrospray mass spectrometry. With, the europium complex of L^3, for example, the anion adduct [EuL^{3}H(CO$_3$)Na$_3$]$^+$ was observed at *m/e* 1089 D for aqueous methanolic solutions of the complex, in the presence of sodium carbonate. The differing pH values for the stability constant determinations were chosen after examining the pH dependence of the single anion solution titrations; a pH value was chosen around which pH-based modulation of emission intensity was minimal.

Similar series of experiments were carried out for [EuL^1] and [EuL^2], (Table 2). The order of complex affinity for lactate and bicarbonate was of the same order of magnitude, with ternary anion adducts of L^1 being weakest and those of L^3 being the strongest. This affinity order may simply reflect the lesser free energy of hydration of the complexes, with the more hydrophobic ligands in [EuL^2] and [EuL^3]. No spectral evidence for the binding of citrate by [EuL^2] and [EuL^3] could be obtained. In each of these

Table 2 Summary of anion binding affinity constants[a], log K_{EuLX}, at the stated pH (0.1 M NaCl, 295 K) and pK_a values associated with *N*-sulfonamide protonation for [EuL^n], (n = 1,2,3)

Complex	Lactate[b] (pH 5.5)	Citrate[c] (pH 7.4)	Bicarbonate (pH 7.4)	pK_a (±0.1) (*N*-sulfonamide)
[EuL^1]	3.50(0.06)	4.59(0.05)	1.97(0.03)	6.1
[EuL^2]	3.86(0.02)	< 1	2.15(0.02)	7.6
[EuL^3]	4.09(0.08)	< 1	2.75(0.02)	6.2[d]

[a] Standard deviations are given in parentheses. [b] Lactate affinities at pH 7.4 were not assessed here as the Eu emission profile (2.3 mM lactate background) was steeply pH dependent over the range 6 to 8 for each complex. [c] Over the pH range 3.3 to 8.0, in the presence of 2 mM sodium citrate, no evidence for citrate binding was found for [EuL^2] and [EuL^3] and only spectral changes associated with sulfonamide N-ligation or (for [EuL^2]) intramolecular coordination of the terminal glutarate carboxylate group were observed. At pH 6.5, [EuL^1] gave an apparent affinity constant of 4.73 (±0.04). [d] In the presence of 0.7 mM human serum albumin, this value is 7.2 (±0.07).

complexes, both electrostatic repulsion and the enhanced steric demand about the Eu centre may suppress citrate ligation. For [EuL^1], however, citrate binding occurred readily and at pH 6.5 an affinity constant of 4.73 was calculated, monitoring changes in the ratio of the 614/612 nm bands (Fig. 4). A similar value was obtained by examining the modulation of the 680/694 nm intensity ratio. It is pertinent to note here that the affinity for citrate in such europium complexes may be enhanced in analogous positively charged complexes, for which greater binding selectivity over lactate is also a feature.[19b,23]

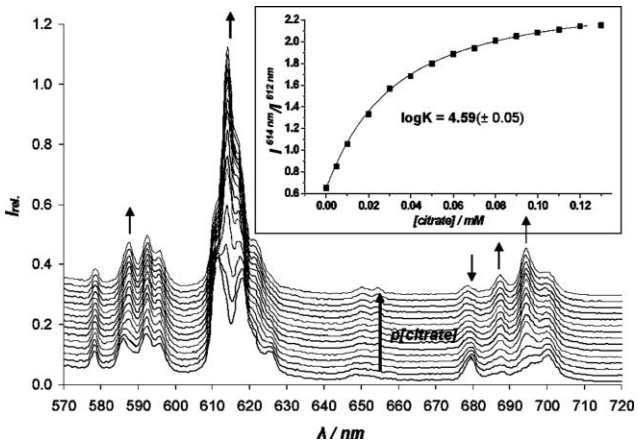

Fig. 4 Variation of the emission spectrum of [EuL^1] with added sodium citrate, allowing an estimation of the 1 : 1 anion formation constant (pH 7.4, λ_{exc} 380 nm, 0.1 M NaCl, 298 K, [complex] = 20 μM).

Protein affinity of [EuL^3]

At this stage, only the complex [EuL^3] was selected for further studies. Each of the other complexes had drawbacks as a pH probe. [EuL^1] suffered significant interference from hydrogen carbonate and lactate or citrate. In the former case, this was most evident over the range 8 to 6.5 suppressing the desired intramolecular sulfonamide binding, with lactate or citrate, interference was most apparent below pH 6.5. For [EuL^2], the introduction of the glutarate groups did inhibit intermolecular anion binding to some extent. However, the competition between intramolecular carboxylate binding (pH range 4 to 7), reversible hydrogen carbonate binding (pH 6.5 to 8) and the desired intramolecular sulfonamide coordination meant that spectral changes were rather complex and were less well defined than the pH-emission response profile of [EuL^3].

Protein interference was examined using human serum albumin. This 66 kD protein is known to possess one high affinity site for aryl substrates and 4 other binding sites of much reduced affinity.[24] The affinity of the lanthanide complex for the protein was assessed by a spectral titration with the Eu complex and by monitoring changes in relaxivity with added protein for the Gd analogue. Titrations were carried out using either aqueous 0.1 M NaCl solution as the background medium or the simulated extracellular anion mixture at pH 7.4 (±0.05). Changes in both ligand fluorescence (440 nm) and Eu emission (570–720 nm) were monitored as a function of added protein concentration. During each of these titrations, significant structural changes in europium emission were not observed. Therefore, the concept

of direct binding of any of the protein's functional groups to the Eu centre can be eliminated. Interestingly, with increasing protein concentration, the ratio of ligand fluorescence *versus* Eu emission intensity did change significantly. This change involved a significant decrease in the intensity of ligand fluorescence at 440 nm following addition of HSA. This may be attributed to quenching of the chromophore fluorescence (azathiaxanthone S_1 state) by electron transfer from the electron rich aromatic groups in HSA, such as Tyr or Trp. However, a mechanism involving energy transfer may also be possible.

The protein affinity of [EuL^3] can be described by an apparent binding constant, assuming a 1 : 1 stoichiometry, consistent with the well known propensity of HSA to form stable complexes with certain annulated aromatics in the 'high affinity' type IIa binding site.[24] Values for log $K = 4.46$ (± 0.03) and 4.21 (± 0.02) were calculated from the intensity ratio 440/612 nm *versus* [HSA] plot, using the extracellular anion medium and 0.1M NaCl solution as background, respectively.

The relaxivity of [GdL^3] in the presence of 0.7 mM HSA in water, was measured to be 3.1 mM^{-1} s^{-1} at pH 3 (37 °C, 60 MHz). Increasing the pH to 7.5 caused the relaxivity to rise to 14.2 mM^{-1} s^{-1}. Further increases in pH caused no significant relaxivity change. The inverse experiment (pH 9 to 3) gave the same result with ±5% fluctuation in the observed relaxivity values (Fig. 5). Repetition of this study, using the mixed extracellular anion solution as background, did not alter the values obtained significantly. The 'relaxivity' titration (pH 7.4, 310 K), monitoring the change as a function of added HSA gave a similar binding constant (Fig. 5) in 0.1 M NaCl (log $K = 4.14$ (± 0.07)) and in the mixed anion medium (log $K = 4.22 \pm 0.05$). These values are the same within error, as those obtained (log $K = 4.21$ (± 0.03) by the luminescence titration at 298 K, and are consistent with reversible binding of the lanthanide complex to the protein with predominant formation of a 1 : 1 adduct.

Use of [EuL^3] in microscopy and spectroscopy for determination of cellular pH

A series of emission response *vs.* pH curves was examined to define the ratiometric profile of the europium complex [EuL^3], in fluids of varying composition. These were in order of increasing complexity: 0.7 mM HSA in 0.1 M NaCl solution; 0.7 mM HSA in the anion mixture with either 5 mM or 30 mM [HCO_3^-]); reconstituted human serum solution (100%), (Fig. 6). Analyses of the variation of the 680/589 nm intensity ratio with pH were broadly similar, with an apparent protonation constant of 7.2 (± 0.1) in each case. Not only the protonation constant was altered upon protein binding, but also there was a significant increase in the Eu radiative lifetime at pH 7.4. The measured overall emission quantum yield increased to 14% (100% increase). This behaviour may be attributed to a perturbation of the energy of the sensitiser S_1 and T_1 states following protein binding, accompanied by increased shielding of the sensitiser excited states from vibrational deactivation. As a consequence, the rate of energy transfer between

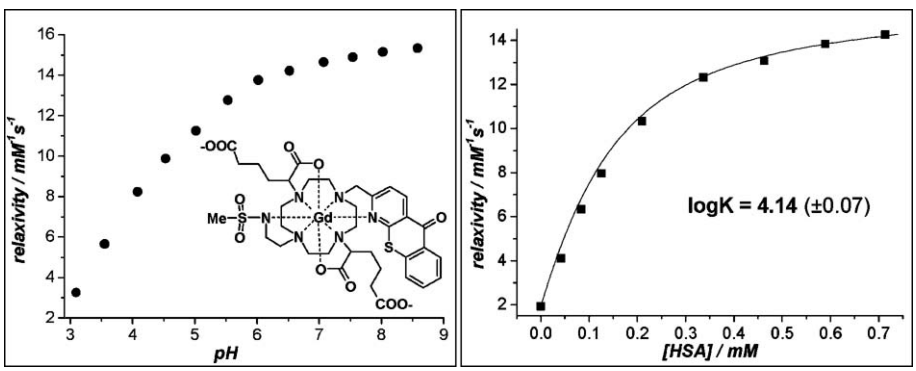

Fig. 5 left: Variation of the relaxivity of [GdL^3] with pH in the presence of 0.7 mM HSA in water; *right*: change in the measured relaxivity with added protein concentration, showing the fit (line) to the observed data for a 1 : 1 binding model (310 K, 60 MHz, $I = 0.1$ M NaCl, [complex] = 90 μM).

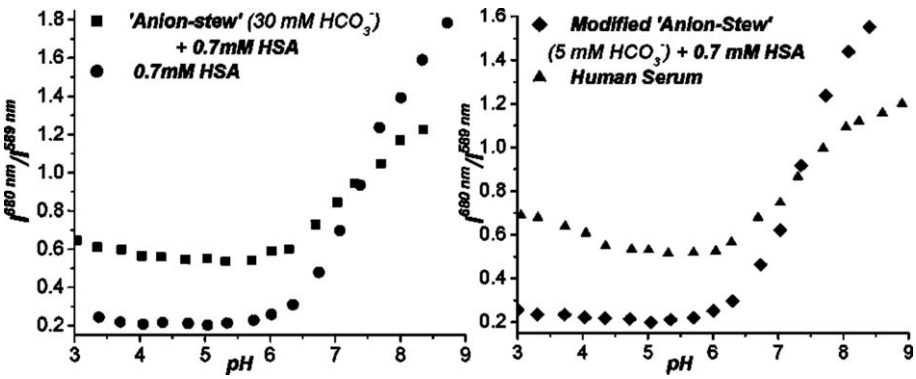

Fig. 6 Europium emission intensity ratio *vs.* pH plots for [EuL^3] using the stated medium (298 K, 0.1 M NaCl, $\lambda_{exc} = 380$ nm, [complex] = 20 mM); *squares*: 0.7 mM HSA plus simulated extracellular anion mixture (30 mM [HCO_3^-]); *circles*: 0.7 mM HSA only; *diamonds*: 0.7 mM HSA plus simulated extracellular anion mixture (5 mM [HCO_3^-]); *triangles*: reconstituted human serum solution.

the sensitising chromophore and the Eu $^5D_0$ state excited state may also become more efficient.

An attempt was made to demonstrate the applicability of [EuL^3] to pH measurement. Spectroscopic analysis can be used when an extracellular pH determination is required, simply by obtaining a small volume of the fluid and measuring the emission intensity ratio of the sample. This analysis requires a high resolution spectrofluorimeter and an appropriate pH calibration curve for the complex in the relevant medium. However, for *in cellulo* applications a different approach is required. One such application, involves the use of a fluorescence microscope, with suitable excitation wavelength and emission filters for observing the total Eu emission and the ligand fluorescence. More importantly, for pH measurements, filters dedicated to observation of individual ΔJ manifolds are required. Therefore, with the incorporation of a fibre optic into the microscope set-up, measurement of different 'areas' of the Eu emission is possible for a given cell or cell compartment, in which the complex localises. Consequently, instead of measuring peak intensity ratios, selected 'area' ratios of the Eu emission can be plotted as a function of pH. This analysis requires that the ratio of the integrated changes, in a selected manifold, is proportionate to the changes of its constituent bands.

A calibration curve was obtained (Fig. 7) using the ratio defined by ($1/\Delta J = 2)/\Delta J = 4$) manifolds (*i.e.* [1/618–628 nm]/678–689 nm) (Fig. 7). By plotting the intensity ratio of the europium emission bands spanning 621–626 nm *versus* 681–687 nm, a 250% change in this parameter was obtained between pH 6 and 8.

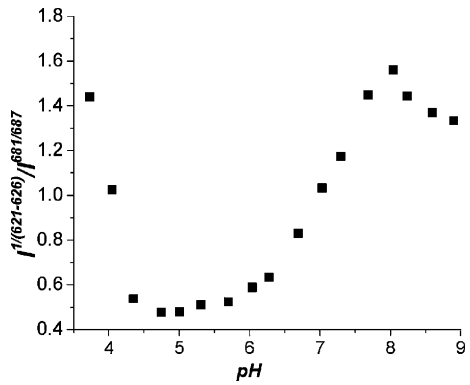

Fig. 7 'Area' ratio (1/618–628 nm)/678–689 nm *versus* pH plot for [EuL^3] using reconstituted human serum solution ([complex] = 20 μM, 298 K, $\lambda_{exc} = 380$ nm, $I = 0.1$ M NaCl).

Behaviour of [EuL^3] in NIH 3T3 cells and assessment of intracellular pH

The cellular uptake profile of the complex [EuL^3] was examined in mouse embryonic fibroblast (NIH 3T3) cells, which were grown in a monolayer on 0.1 mm thick glass cover slips. Incubation times varied from 1 to 24 h, while two different complex concentrations were loaded onto the cells (50 and 100 μM) by dissolving lyophilised complex in Dulbecco's Modified Eagle Medium (DMEM) containing 10% NCS (Newborn Calf Serum) and 1% penicillin–streptomycin. Prior to mounting of the cells without any additional treatment, incubation was carried out for each individual time point in a copper jacketed incubator using 5% CO_2 and about 10% relative humidity. Cover slips were mounted, by withdrawal of the growth medium, subsequent washing with phosphate buffered saline (PBS) solution (×3) followed by sealing them around the edge onto the 1 mm thick microscope slide. The uptake and distribution of the complex within the cell was observed by fluorescence microscopy, following excitation of the chromophore.

Epifluorescence images were taken on a Zeiss Axiovert 200M epifluorescence microscope. For excitation a 340–390 nm (90% transmission) band-pass (BP) filter was used. Ligand fluorescence was observed using a 445–465 nm band-pass filter (80% transmission), while Eu emission was observed using a 570 nm long-pass (LP) filter (85% transmission). Confocal microscopy images were taken on a Zeiss LSM 500 META confocal microscope using a BIORad 405 nm diode laser for excitation, with appropriate filters to allow ligand fluorescence or europium emission to be observed.

Incubation of NIH 3T3 cells with [EuL^3] resulted in fluorescence that could be readily detected. For each time point (2, 4, 6, 8, 10, 12, 24 h), epifluorescence and confocal images were recorded; the former images were taken immediately, whilst confocal images were recorded in each case after the 24 h time point. When optical sections through the cells were taken, the fluorescence could be detected in each layer. This confirms that the complex has been successfully taken up into the cells, and was not merely associating with the cell membrane. As a control, untreated cells were mounted and they showed no fluorescence in each of the observed wavelength regions. While only one set of images for each time point is shown here, images were taken at a number of points across the slide, with a similar localisation profile observed at each position.

Two different loading concentrations were applied, 50 μM and 100 μM. Each provided bright images, with no significant concentration dependence in image quality and more importantly, localisation profile. Images recorded at 30 min and 1 h showed similar localisation profiles, with lower overall fluorescence intensity. Therefore, longer acquisition times were required, which led to some image distortion. No time dependence for either ligand or Eu emission intensity was observed in the 2 to 12 h loading period, and neither were significant changes observed in complex localisation. This effect was studied, by comparing the acquisition time of constant overall brightness of each recorded image containing a constant number of cells and as a function of complex loading time (Fig. 8). The colour consistency of the merged images suggests that the complex remains chemically inert and no evidence for complex dissociation was apparent within the cells; *i.e.* separate ligand fluorescence was not observed.

By analysing each image recorded, there appears to be complex localisation in the protein-rich regions of the nucleolus, with localisation in other organelles in the cytoplasm. The appearance of these organelles is most consistent with the size and distribution of the protein-dense ribosomes. As the images revealed a more intense fluorescence around the nuclear membrane, it is also possible that there is some degree of perinuclear localisation. However, the light intensity of the nucleoli was found to be 2.8 times higher than that in the cytoplasm and 1.5 times higher than in the nuclear membrane (Fig. 9). This intensity differentiation permits the acquisition of an exclusive image of the nucleolus by adjusting the excitation intensity or the gain of the microscope (acquisition time).

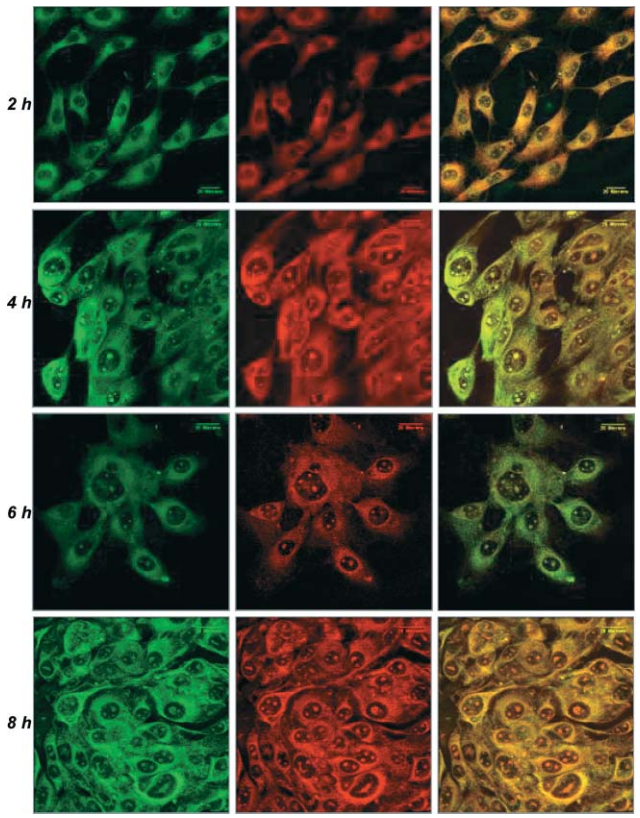

Fig. 8 Confocal fluorescence microscopy images of NIH 3T3 cells (mouse skin fibroblasts) loaded with [EuL^3] (2, 4, 6 and 8 h incubation 100 μM complex concentration in the growth medium), $\lambda_{exc} = 405$ nm, observing Eu emission above 570 nm (*red*) and azathiaxanthone fluorescence (*green*) at 450 nm separately and merged (right), revealing the localisation of the complex in the nucleolus and showing the ribosomal profile in the extranuclear regions.

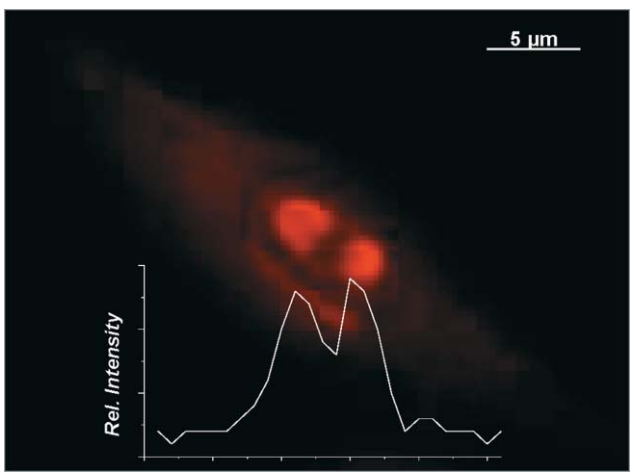

Fig. 9 Fluorescence microscopy images of EuL^3 (λ_{ex} = BP 340–390 nm, λ_{em} = LP 570) in an NIH 3T3 cell, with integration of the light intensity, highlighting the localisation of the complex in the nucleoli.

The number of nucleoli in the cell depends on its mitotic stage and its health status. The nucleolus is visible before mitosis (interphase), dissolves at prophase, and then becomes discernible again at telophase.[25] As is evident from the images, almost every cell examined has more than two nucleoli. This is consistent with the fact that NIH 3T3 cells, like more malignant cells, possess a higher nucleolus number, a feature that is related to their cell proliferative activity.[26] This hypothesis for localisation was based on similar observations, with a structurally related europium complex, [EuL^4]$^{3+}$, that possesses the same coordinating sensitiser, and also binds strongly to protein.[23] Cell viability was found to be concentration and time dependent, and was monitored by visual counting of the number of cells in a selected population as a function of time. From bright field measurements, more than 95% of the cells were considered to be healthy over the 24 h period. An MTT cell toxicity assay[27] indicated that the IC_{50} value was >>67 (±19) μM.

For determination of the [EuL^3] concentration in the cells, an 8 h loading time point with a 100 μM loading concentration was chosen. Not only the sorted and counted (201 794) cells were submitted for ICP-MS, but also the combination of PBS washings used after growth medium withdrawal. The number of Eu complexes inside a single cell was determined to be 2.9×10^7. This value gives a $[Eu]_{total}$ of 12.5 μM inside a single cell (assuming 4000 μm^3 as the mean cell volume), which means that 12.5% of the original loading concentration had been taken up by the cells. This measurement was confirmed by comparing the absorbance values of the complex containing growth medium prior to and after incubation, giving a 14% (±2%) decrease in complex concentration. Surprisingly, 31% of the complex concentration measured by ICP-MS was measured from the submitted PBS solution. This not only confirms the observed relatively fast influx of the complex, but warns about rapid egress, upon withdrawal of complex from the growth medium. Although time dependent egress experiments were not carried out in this work, this behaviour is consistent with a diffusion-driven transport mechanism across the cell membrane. The driving force of this hypothetical mechanism is the complex concentration gradient between the intracellular and extracellular space. This also supports the observed time independent complex uptake profile, noted in the fluorescence microscopy studies.

In an attempt to utilise the pH-mapping function of the complex, NIH 3T3 cells loaded with 50 μM complex were used in a trial experiment. Fast egress of Eu(III)complexes designed for *in cellulo* applications had been observed. Withdrawal of the medium containing the complex leads to relatively fast egress of the complex from the cells. Therefore, cells were removed from their growth medium containing the complex, and quickly washed three times with PBS. Cells were suspended in PBS following scraping them into a fluorescent cuvette (detaching them from the surface using trypsin takes 5 min, with additional washes using PBS) and measuring the emission spectrum. This process was completed within a minute, to ensure minimal release of complex from the cells.

In the absence of an appropriate calibration curve in simulated intracellular mouse skin fibroblasts, the intensity ratio *vs.* pH plot for [EuL^3] in reconstituted 100% human serum was used (Fig. 7). Due to the descending baseline of the spectrum caused by ligand fluorescence and light scattering, subtraction of the ligand fluorescence from the Eu emission spectrum was used, prior to analysis of the 680/617.5 nm intensity ratio. Estimation of the pH, using the measured intensity ratio of 0.138, gave a global pH within the cell of 7.4. Evidently, the error of this measurement is relatively high (±0.2). In order to confirm this, a large number of cells (*ca.* 20 000) with the same loading concentration and time were removed mechanically from their cover-slips, washed with

PBS (×3), and subsequently sonicated to achieve a homogenous macerated cell solution (50 μL). The emission spectrum of this sample was recorded, albeit with low resolution due to the small sample volume. A pH of 7.6 (±0.1) was obtained using the usual intensity ratio. For comparison, the pH of the solution was also measured using a narrow, accurately calibrated electrode, giving a pH value of 7.47 (±0.05).

These trial experiments carry a number of assumptions. They do, however, support the application of [EuL^3] as a ratiometric pH probe, capable of estimating intracellular pH.

Summary and conclusions

A series of pH-responsive ratiometric Eu(III)complexes has been synthesised incorporating an efficient sensitiser and a pH dependent binding moiety. Their luminescence properties were thoroughly studied to identify the best candidate for intra- and extracellular pH measurements. The complex, [EuL^3] exhibited some interference from endogenous anions and protein. Despite this, even using reconstituted 100% human serum, a suitable calibration curve was obtained and was applied to determine the local pH using intensity ratio *vs.* pH plots for spectroscopic applications. Selected emission band ratio *vs.* pH plots allow application of this method to microscopy, measuring pH over the range 6 to 8 using an appropriate microscope set-up.

Cellular uptake images revealed fast uptake of the complex and a well distributed localisation within the cell. However, fast egress was also observed. Ribosomal localisation with an even higher concentration within the nucleoli was observed, in a similar manner to structurally related complexes bearing the same coordinated sensitising moiety. The localised complex seems to remain intact within the cell, and an IC_{50} value of 67 (±19) μM was measured using the MTT[27] cell toxicity assay. Images were observed using non-fixed cells, which is appropriate for live cell imaging applications. Thus, this complex shows promise for application as a ratiometric intracellular pH probe for living cells and related biological media.

Experimental

All commercially available reagents were used as received, from their respective suppliers. Solvents were dried using an appropriate drying agent when required (CH_3CN over CaH_2, CH_3OH over $Mg(OMe)_2$ and THF over Na–benzophenone). Water and air sensitive reactions were carried out under argon atmosphere. Water and H_2O refer to high purity water with conductivity ≤0.04 μS cm^{-1} obtained from the 'Purite$_{STILL}$ Plus' purification system. Thin-layer chromatography was carried out on neutral aluminium oxide plates (Merck Art 5550) or silica plates (Merck 5554), both visualised under UV irradiation (254 nm) or iodine staining. Preparative column chromatography was carried out using neutral aluminium oxide (Merck Aluminium Oxide 90, activity II–III, 70–230 mesh), pre-soaked in ethyl acetate, or silica (Merck Silica Gel 60, 230–400 mesh). Melting points were measured using a Reichart-Kofler block and are uncorrected.

^{1}H and ^{13}C NMR spectra were recorded on a Varian Mercury 200 (^{1}H at 199.97 MHz, ^{13}C at 50.29 MHz), Varian Unity 300 (^{1}H at 299.91 MHz, ^{13}C at 75.41 MHz), a Varian VXR 400 (^{1}H at 399.97 MHz, ^{13}C at 100.57 MHz), a Bruker Avance spectrometer (^{1}H at 400.13 MHz, ^{13}C at 100.61 MHz), or a Varian Inova-500 (^{1}H at 499.78 MHz, ^{13}C at 125.67 MHz). All spectra were referenced internally to the solvent residual proton signals, except for complexes in D_2O, where *tert*-butanol was added as an internal reference ($\delta = 0$ ppm).

Electrospray mass spectra were recorded on a VG Platform II (Fisons Instrument), operating in positive or negative ion mode as stated, with methanol as the carrier solvent. Accurate masses were measured on a Thermo Finnigan LQT. UV/Vis absorbance spectra were recorded either on a Perkin Elmer Lambda 900 UV/Vis/NIR spectrometer (using FL Winlab software) or a Unicam UV/Vis UV2. Emission spectra were measured on a ISA Joblin-Yvon Spex Fluorolog-3 luminescent spectrometer (using DataMax v2.20 software), while lifetimes were measured on a Perkin Elmer LS55 luminescence spectrometer (using FL Winlab software). All samples were contained in quartz cuvettes with a path length of 1 cm and polished base. Measurements were obtained relative to a reference of pure solvent contained in a matched cell.

Luminescent titrations were carried out by normalising the emission spectra with the absorption spectra at each point in order to revise the decrease in the sample concentration caused by pH adjustment or addition of an anion/cation stock solution where appropriate. All measurements were carried out using $I = 0.1$ M NaCl ionic background.

Relaxivity measurements were carried out at 37 °C and 60 MHz on a Bruker Minispec mq60 instrument. The mean value of three separate measurements was recorded and averaged.

pH metric titrations were monitored using a Jenway 3020 or a Jenway 3320 pH meter attached to an Aldrich Chemical Company micro-pH combination electrode (three point calibration using pH = 4.0 ± 0.02, pH = 7.00 ± 0.02 and pH = 10.00 ± 0.02 (T = 20 °C) buffer solution supplied by Aldrich. The adjustment of pH was carried out using conc. NaOH and conc. HCl (or NaOD and DCl if required) solution to avoid any significant increase in sample volume. For measurements carried out in D_2O the pD was calculated using the actual pH meter reading and the equation:[28,29] pD = pH (meter reading) + 0.41.

Lifetimes of europium complexes were measured by excitation of the sample using a short pulse of light (380 nm or 384 nm depending on the nature of the complex) followed by monitoring the integrated intensity of light (for europium 612–618 nm depending on the measured species and the pH) emitted during a fixed gate time, t_g, after a delay time, t_d. At least 20 delay times were used covering 3 or more lifetimes. A gate time of 0.1 ms was used, and the excitation and emission slits were set to 10 nm and 2.5 nm band-pass respectively. The obtained exponential decay curves were fitted to the equation below, using Origin 6.0 software (Data Analysis & Technical Graphics):

$$I = A_0 + A_1\exp(-kt)$$

To examine the influence of some biologically common anions on Eu complexes, luminescent titrations were carried out by using an 'anion stew', containing 30 mM Na_2CO_3, 2.3 mM Na(lactate), 0.9 mM NaH_2PO_4 and 0.13 mM Na_3(citrate) to assess the overall influence of these anions. Luminescence titrations were also carried out by using the above-mentioned anions separately along with [ascorbate] = 0.3 mM and [HSA] = 0.7 mM, in order to study their individual effect on the Eu emission spectra. Each

measurement was carried out using a constant $I = 0.1$ M NaCl ionic strength. Titrations were carried out from basic solutions with acidification in order to avoid the undesirable evolution of carbon dioxide. As the studied Eu-complexes showed major changes in their Eu emission spectrum in the presence of some biologically common anions, the concentration dependence of the Eu emission was examined. A series of measurements was carried out with the Eu-complexes presented in this work by applying the appropriate anions that caused significant spectral changes in the Eu emission at a chosen pH where the anion influence was maximised within the relevant pH-range. All of these measurements were carried out by adding the selected anion as liquid concentrated stock solution where the addition at each point was approx. 0.1–0.5% in volume of the original solution observed to avoid significant increase in sample volume. HSA was added as a solid. Each Eu emission spectrum was corrected for dilution. The apparent binding constant of the selected anion was calculated using the equation below:

$$[\mathrm{X}] = \frac{[(F-F_0)/(F_1-F_0)]/K + [\mathrm{EuL}](F-F_0)/(F_1-F_0)}{1-(F-F_0)/(F_1-F_0)} - \frac{[\mathrm{EuL}][(F-F_0)/(F_1-F_0)]^2}{1-(F-F_0)/(F_1-F_0)}$$

where: [X]: the total concentration of anion in the solution; [Eu]: the total concentration of the complex; K: the binding constant; F: the ratio of selected peaks; F_0: the initial ratio; F_1: the final ratio; [EuX]: the concentration of the anion-coordinated complex; [X_f]: the concentration of free anion in the mixture; [Eu_f]: the concentration of the free complex.

Low temperature phosphorescence spectra measurements were carried out on the chromophores to enable the determination of their triplet state involved in sensitisation. An Oxford Instruments optical cryostat operating at 77 K was used with the samples dissolved in EPA (Et_2O– isopentane–EtOH [2 : 5 : 5 by volume]) and contained in 10 mm cuvettes. The triplet energy was obtained from the extrapolation of the highest energy (shortest wavelength) phosphorescence band, corresponding to the 0–0 transition, using time-gated detection.

Microscopy

Epifluorescence images were taken on a Zeiss Axiovert 200M epifluorescence microscope with objectives 63×/1.40 oil DIC and 40×/1.40 oil DIC respectively, equipped with an Axiocam CCD camera. For excitation a 340–390 nm (90% transmission) band-pass (BP) filter was used. Ligand fluorescence was observed using a BP 445–465 nm filter (80% transmission), while Eu emission was observed using a 570 nm long-pass (LP) filter (85% transmission). Confocal images were taken on a Zeiss LSM 500 META confocal microscope with a BIORad 405 diode laser excitation and an LP 590 nm emission filter were used for europium luminescence and a BP 505–550 filter for study of ligand fluorescence.

Cell culture and toxicity

Two cell lines were selected for cell cultural studies CHO (Chinese hamster ovary) cells and NIH 3T3, mouse skin fibroblast (connective tissue) cells. Each line is transformed, and comprise adherent cells, which grow in a monolayer. These cell lines were cultured in a copper jacket incubator at 37 °C, average 20% humidity and 5% (v/v) CO_2 in 50 mL volume plastic grow plates. Cells for microscopy were grown in a 24 well-plate using $d = 13$ mm glass cover slips (average thickness $l = 0.1$ mm). DMEM (Dulbecco's Modified Eagle Media), and F-12(Ham) media were used for NIH 3T3 and CHO cells respectively, each containing 10% (v/v) NCS (Newborn Calf Serum) and 1% (v/v) penicillin-streptomycin. Complexes were loaded onto cells using the appropriate growth medium. For flow cytometry measurements, cells were detached from the glass surface using 1% (v/v) trypsin solution at 37 °C for 5 min. The solutions and washings were analysed in separate ICP-MS measurements to measure any possible europium complex egress.

IC_{50} values were determined using the MTT assay, as described by Carmichael *et al.*[27] which makes use of the conversion of MTT (3-(4,5-dimethylthiazol-2-yl)-2,5-diphenyltetrazolium bromide) to a purple formazan product by the mitochondrial dehydrogenase of viable cells. This insoluble formazan was quantified spectrophotometrically upon dissolution in DMSO. Approximately 5×10^3 NIH 3T3 cells in 100 μL DMEM were seeded into each well of flat-bottomed 96-well plates and allowed to attach overnight. Complex solutions were added to triplicate wells to give final concentrations over a 2-log range. Following 24 h incubation, MTT (1.0 mM) was added to each well, and the plates incubated for a further 4 h. The culture medium was removed, and DMSO (150 μL) was added. The plates were shaken for 20 seconds and the absorbance measured immediately at 540 nm in a microplate reader. IC_{50} values were determined as the drug concentration required to reduce the absorbance to 50% of that in the untreated, control wells, and represent the mean for data from three independent experiments. Observations of cell viability using bright field microscopy suggested that for [EuL^3] at both 50 and 100 μM loading concentrations, no obvious changes in cell shape/morphology had occurred.

Flow cytometry and inductively coupled plasma mass spectrometry

Flow cytometric analysis and sorting was conducted using a DakoCytomation Inc.MoFlo multi-laser flow cytometer (Fort Collins, CO, USA) operating at 60 psi, 70 micron nozzle. Samples were interrogated with a 100 mW 488 nm solid state laser: (FSC, SSC). Fluorescence signals were detected through interference filters FL1 530/40, FL2 58030, FL3 630/30 and FL4 670/30). Fluorescence signals were collected in logarithmic mode. The data were analyzed using Summit v4.0 (DakoCytomation) software. ICP-MS determination of europium concentrations from cells and growth media were carried out by Dr Chris Ottley in the Department of Earth Sciences at Durham University using a Thermo Finningan ELEMENT$_2$ High Resolution Select Field ICP-MS.

HPLC analysis/purification

Reverse phase HPLC analyses were performed at 298 K on a Perkin Elmer system using a 4.6 × 20 mm 4 μ Phenomenex Synergi Fusion RP 80i analytical column. In each case an H_2O + 0.1% HCOOH–MeCN + 0.1% HCOOH solvent system was used (gradient elution) with a run time of 20 minutes. In each case,

a single major product was observed in >95% purity using a diode array UV-Vis detector operating at 380 mm (analysis was also undertaken at 280 nm). This corresponds to the absorption band of the appropriate azathioxanthone used as sensitising moiety for each Eu-complex and is at a longer wavelength than any organic contaminant. Such behaviour indicated that each of the species that was eluted bore this chromophore. A fluorescence detector was also connected to the HPLC, monitoring eluent from the column at a wavelength corresponding to the Eu centered emission (616 nm); again emission was seen for each of these peaks, suggesting that each peak corresponding to a chromophore bound species also was coordinated to Eu in such way that it was efficiently sensitised. For each Gd complex, a UV-Vis detector was used operating with a LP 250 nm detection filter.

Ligand and complex synthesis

4-[(1-Azathioxanthone)-2-methyl]-1,7-bis(*tert*-butoxycarbonylmethyl)-1,4,7,10-tetraazacyclododecane.

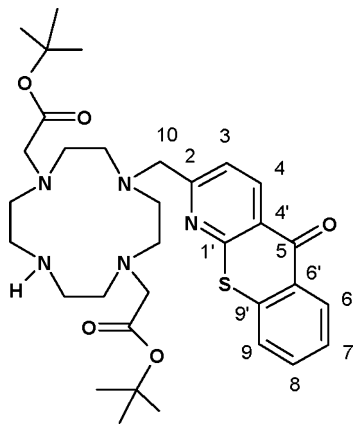

1,7-Bis(*tert*-butoxycarbonylmethyl)-1,4,7,10-tetraazacyclododecane (250 mg, 0.62 mmol) was combined with 2-bromomethyl-1-azathiaxanthone (1.1 eq., 190 mg) and K_2CO_3 (1 eq., 86 mg) and the mixture stirred in dry MeCN (12 mL) at reflux under argon for 18 h. The reaction was monitored by TLC (DCM : MeOH, 97 : 3) and $ESMS^+$ to confirm that the brominated starting material had been consumed. The solvent was removed under reduced pressure. The resulting solid was dissolved in a small volume of DCM (5 mL) and the $KBr–K_2CO_3$ was filtered out. The crude mixture was purified by column chromatography (DCM→2% MeOH) to yield the title compound as a yellow oil (161 mg, 0.26 mmol, 42%). δ_H ($CDCl_3$) 8.71 (1H, H^4, d, *J* 8.1 Hz), 8.60 (1H, H^6, d, *J* 8.0 Hz), 7.68 (2H, $H^{8,9}$, m), 7.49 (1H, H^7, m), 7.30 (1H, H^3, d, *J* 8.1 Hz), 3.87 (2H, H^{10}, s), 3.13–2.78 (4H, CH_2CO_2 + 16H, NCH_2CH_2N, m), 1.42 (18H, ^{t}Bu, s); δ_C ($CDCl_3$) 180.7 (C^5), 170.2 ($CO_2{}^t$Bu), 161.3 (C^2), 158.6 ($C^{1'}$), 139.2 ($C^{4'}$), 137.5 ($C^{6'}$), 133.3 (C^8), 130.2 (C^6), 129.3 ($C^{9'}$), 127.5 (C^7), 127.1 (C^9), 124.8 (C^4), 122.2 (C^3), 80.9 (CMe_3), 52.4 (C^{10}), 57.9 (CH_2CO_2), 50.1, 47.8 (NCH_2CH_2N), 27.8 (CH_3); *m/z* ($ESMS^+$) 626 (M + 1); R_f 0.18 (DCM–3%MeOH, alumina).

4-[(1-Azathioxanthone)-2-methyl]-10-[2-(methylsulfonylamino)ethyl]-1,7-bis(*tert*-butoxycarbonylmethyl)-1,4,7,10-tetraazacyclododecane.

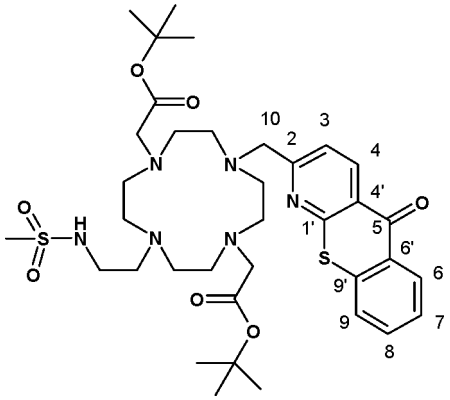

4-[(1-Azathioxanthone)-2-methyl]-1,7-bis(*tert*-butoxycarbonylmethyl)-1,4,7,10-tetraazacyclododecane (87 mg, 0.14 mmol) was combined with *N*-methanesulfonylaziridine (1.1 eq., 17.3 mg) and K_2CO_3 (1 eq., 19 mg) stirred in dry MeCN (8 mL) at reflux under argon for 24 h. The reaction was monitored by TLC (DCM : MeOH, 97 : 3) and $ESMS^+$ to confirm that the starting secondary amine had been consumed. The solvent was removed under reduced pressure. The resulting solid was dissolved in a small volume of DCM (3 mL) and the K_2CO_3 was filtered out. The crude mixture was purified by column chromatography on neutral alumina (DCM→2% MeOH) to yield the title compound as a light brown oil (72 mg, 97 μmol, 69%). δ_H ($CDCl_3$) 8.71 (1H, H^4, d, *J* 8.0 Hz), 8.60 (1H, H^6, d, *J* 8.0 Hz), 7.68 (2H, $H^{8,9}$, m), 7.49 (1H, H^7, m), 7.31 (1H, H^3, d, *J* 8.0 Hz), 3.90 (2H, H^{10}, s), 3.13–2.78 (4H, CH_2CO_2 + 16H, NCH_2CH_2N + 4H, $SO_2NHCH_2CH_2N$ m),), 2.01 (3H, SO_2CH_3), 1.41 (18H, ^{t}Bu, s); δ_C ($CDCl_3$) 180.7 (C^5), 170.2 ($CO_2{}^t$Bu), 161.3 (C^2), 158.6 ($C^{1'}$), 139.2 ($C^{4'}$), 137.5 ($C^{6'}$), 133.3 (C^8), 130.2 (C^6), 129.3 ($C^{9'}$), 127.5 (C^7), 127.1 (C^9), 124.8 (C^4), 122.2 (C^3), 81.1 (CMe_3), 67.0, 67.8 ($SO_2NHCH_2CH_2N$), 52.4 (C^{10}), 57.9 (CH_2CO_2), 50.1, 47.8 (NCH_2CH_2N), 38.5 (SO_2CH_3), 27.8 ($C(CH_3)_3$); *m/z* ($ESMS^+$) 746 [M + 1], 768 [M + Na]; R_f 0.44 (DCM : MeOH, 97 : 3; alumina)

4-[(1-Azathioxanthone)-2-methyl]-10-[2-(methylsulfonylamino)-ethyl]-1,7-bis(carboxymethyl)-1,4,7,10-tetraazacyclododecane.

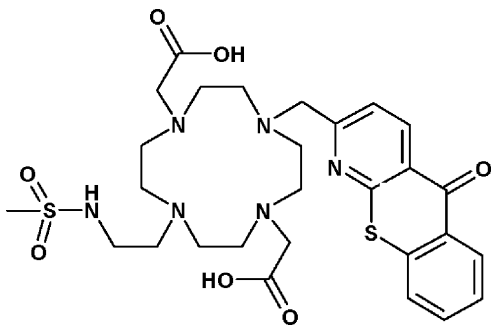

A mixture of trifluoroacetic acid (1.5 mL) and DCM (0.5 mL) was added to 4-[(1-azathioxanthone)-2-methyl]-10-[2-(methylsulfonylamino)ethyl]-1,7-bis(*tert*-butoxycarbonylmethyl)-1,4,7,10-tetraazacyclododecane (72 mg (97 μmol) and the mixture stirred under argon at room temperature for 28 h. The solvents were removed under reduced pressure and a small volume of DCM (3 × 3 mL) was added and removed again under reduced pressure. The crude mixture was dissolved in water (5 mL) and

extracted with DCM (5 mL) thrice, and lyophilised to yield the title compound as a dark orange oil which slowly crystallised (55 mg, 87 μmol, 90%). This material was used for complexation immediately, *m/z* (ESMS$^+$) 658 [M − H + 2Na]; mp 120–121 °C.

EuL^1

4-[(1-Azathioxanthone)-2-methyl]-10-[2-(methylsulfonylamino)-ethyl] - 1,7 - bis(carboxymethyl) - 1,4,7,10 - tetraazacyclododecane (28 mg, 44 μmol) was added to $Eu(CF_3SO_3)_3$ (1.1 eq., 26 mg) and the solids dissolved in MeCN (2 mL) and the reaction stirred at reflux temperature for 30 h. After the reaction was cooled to room temperature the solvents were removed under reduced pressure, the remaining residue was dissolved in 5 mL water : MeOH (5 : 1). The pH was then adjusted carefully to 10 by addition of conc. NaOH solution (in order to get rid of the Eu-excess as $Eu(OH)_3$) resulting in a white precipitates removed *via* a fine syringe filter. The pH was adjusted back to neutral and lyophilised to give a light brown solid, which was loaded onto a DOWEX 1-X8 (Cl) anion exchange resin. The column was eluted with water → 10% NH_4OH and the fractions were analysed by ESMS$^+$. The fractions were combined and lyophilised to yield the Eu-complex as a light brown powder. t_R (HPLC) = 10.3 min; *m/z* (HRMS$^+$) 819.0914 ($C_{28}H_{35}O_7N_6S_2EuCl$ requires 819.0915); $\lambda_{max}(H_2O)$ 380 (4070 M^{-1} cm^{-1}); $\tau_{Eu}(H_2O$, pH = 4.5): 0.48 ms), $\tau_{Eu}(H_2O$, pH = 8.0): 0.41 ms; $\tau_{Eu}(D_2O$, pD = 4.5): 0.76 ms, $\tau_{Eu}(D_2O$, pH = 7.6): 0.48 ms; ϕ_{Eu} (pH = 3.0) = 1%, ϕ_{Eu} (pH = 8.0) = 0.9%.

1,7-Bis(α-dimethylglutarate)-1,4,7,10-tetraazacyclododecane

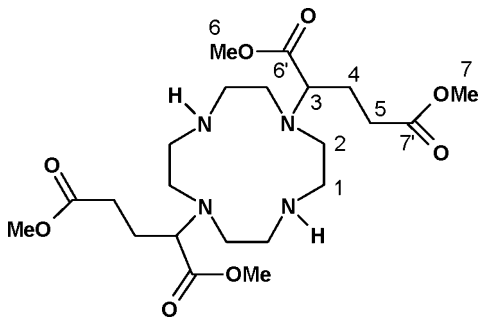

Tetraazacyclododecane (2.00 g, 11.61 mmol), dimethyl 2-bromoglutarate (6.10 g, 25.54 mmol) was dissolved in dry MeCN (20 mL) followed by addition of $NaHCO_3$ (2.14 g, 2.2 eq.). The mixture was stirred at 55 °C under argon. The reaction was monitored by TLC (DCM : MeOH : NH_4OH, 89 : 10 : 1) and ESMS$^+$. After 7 days dimethyl 2-bromoglutarate had been consumed, and the solvent was removed under reduced pressure. The remaining residue was dissolved in DCM (20 mL), the organic layer was washed with HCl (pH 3), dried over K_2CO_3 and the solvents removed under reduced pressure. The residue was purified by column chromatography over silica (DCM : THF : MeOH : NH_4OH, 25 : 65 : 5 : 5). The fractions containing the title product were combined and the solvents were removed under reduced pressure to yield a pale brown oil (1.23 g, 2.52 mmol, 21%). δ_H ($CDCl_3$) 7.68 (2H, br s, NH), 3.63 (6H, s, H^7), 3.57 (6H, s, H^6), 3.26 (2H, m, H^3), 2.78 (16H, m, $H^{1,2}$), 2.36 (4H, m, H^5), 1.92 (4H, m, H^4); δ_C ($CDCl_3$) 173.4 ($C^{7'}$), 172.9 ($C^{6'}$), 64.1 (C^3), 51.9 ($CH_3{}^6$), 51.8 ($CH_3{}^7$), 48.7, 46.5 ($C^{1,2}$), 30.0 (C^5), 22.6 (C^4); *m/z* (ESMS$^+$) 489 [M + 1], 490 [M + 2]; R_f 0.32 (DCM : MeOH : NH_4OH, 89 : 10 : 1, silica).

4-[(1-Azathioxanthone)-2-methyl]-1,7-bis(α-dimethylglutarate)-1,4,7,10-tetraazacyclododecane

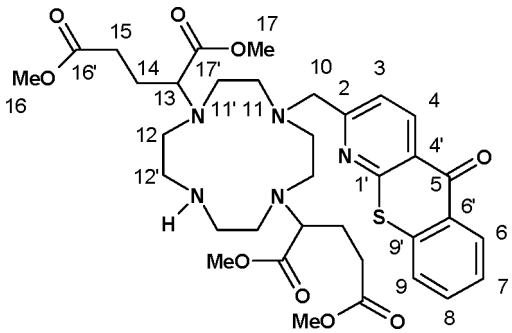

1,7 - Bis(α - dimethylglutarate) - 1,4,7,10 - tetraazacyclododecane (320 mg, 660 μmol) was combined with 2-bromomethyl-1-azathiaxanthone (1 eq., 200 mg) and K_2CO_3 (1 eq., 91 mg) and the mixture stirred in dry MeCN (10 mL) at reflux temperature (85 °C) under argon for 30 h. The reaction was monitored by TLC (DCM : MeOH, 97 : 3) and ESMS$^+$ to confirm that the brominated starting material had been consumed. The solvent was removed under reduced pressure and the resulting solid was dissolved in a small volume of DCM (5 mL) and the KBr–K_2CO_3 filtered out. The crude mixture was purified by column chromatography (DCM→2% MeOH) to yield the title compound as a pale brown oil (120 mg, 168 μmol, 26%). δ_H ($CDCl_3$) 8.68 (1H, d, *J* 8.0 Hz, H^4), 8.43 (1H, m, H^6), 7.59 (2H, m, $H^{8,9}$), 7.42 (1H, m, H^7), 7,24 (1H, d, *J* 8.0 Hz, H^3), 3.83 (2H, s, H^{10}), 3.63 (6H, s, H^{16}), 3.57 (6H, s, H^{17}), 3.26 (2H, m, H^{13}), 2.97 (16H, m, $H^{11,11',12,12'}$), 2.36 (4H, m, H^{15}), 1.92 (4H, m, H^{14}); δ_C ($CDCl_3$) 180.5 (C^5) 173.4 ($C^{16'}$), 172.9 ($C^{17'}$), 161.4 (C^2), 158.6 ($C^{1'}$), 138.4 ($C^{4'}$), 137.5 ($C^{6'}$), 133.3 (C^8), 130.0 (C^6), 129.0 ($C^{9'}$), 127.1 (C^7), 126.6 (C^9), 125.3 (C^4), 122.2 (C^3), 65.1 (C^{13}), 51.9 (C^{17}), 51.8 (C^{16}), 51.3, 50.4, 49.2, 46.5 ($C^{11,11',12,12'}$), 46.1 (C^{10}), 30.9 (C^{15}), 25.7 (C^{14}); R_f 0.16 (DCM : MeOH, 97 : 3; alumina); *m/z* (HRMS$^+$) 714.3163 ($C_{35}H_{48}O_9N_5S$ requires 714.3173).

4-[(1-Azathioxanthone)-2-methyl]-10-[2-(methylsulfonylamino)-ethyl]-1,7-bis(α-dimethylglutarate)-1,4,7,10-tetraazacyclododecane

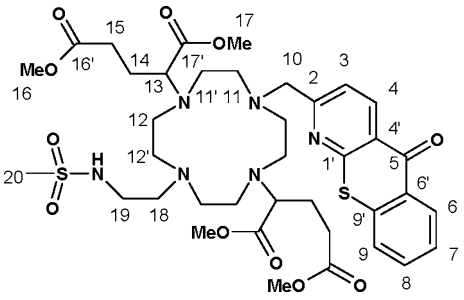

4-[(1-Azathioxanthone)-2-methyl]-1,7-bis(α-dimethylglutarate)-1,4,7,10-tetraaza-cyclododecane (110 mg, 150 μmol) was combined with *N*-methanesulfonylaziridine (1.1 eq., 19.4 mg) and

K_2CO_3 (1 eq., 22 mg) stirred in dry MeCN (5 mL) at reflux temperature (85 °C) under argon for 46 h. The reaction was monitored by TLC (DCM : MeOH, 97 : 3) and $ESMS^+$ to confirm that the starting material had been consumed. The solvent was removed under reduced pressure and the resulting solid was dissolved in a small volume of DCM (3 mL) and the K_2CO_3 removed by filtration. The crude mixture was purified by column chromatography (DCM→2% MeOH) to yield the title compound as a light brown oil which slowly crystallised (50 mg, 60 μmol, 41%). δ_H ($CDCl_3$) 8.70 (1H, d, *J* 8.0 Hz, H^4), 8.48 (1H, m, H^6), 7.63 (2H, m, $H^{8,9}$), 7.44 (2H, d + dd, $H^{3,7}$), 3.83 (2H, s, H^{10}), 3.63 (6H, s, H^{16}), 3.60 (6H, s, H^{17}), 3.26 (2H, m, H^{13}), 3.02 (3H, s, H^{20}), 2.93 (16H, m, $H^{11,11',12,12'}$), 2.50 (6H, m, $H^{15,18}$), 1.90 (4H, m, H^{14}), 1.56 (2H, t, *J* 7.8 Hz, H^{19}); δ_C ($CDCl_3$) 180.5 (C^5) 173.3 ($C^{16'}$), 173.0 ($C^{17'}$), 162.1 (C^2), 158.8 ($C^{1'}$), 138.5 ($C^{4'}$), 137.5 ($C^{6'}$), 133.7 (C^8), 130.0 (C^6), 128.9 ($C^{9'}$), 127.2 (C^7), 126.6 (C^9), 125.5 (C^4), 122.7 (C^3), 65.9 (C^{13}), 51.7 (C^{17}), 51.4 (C^{16}), 54.2, 51.3, 49.2, 46.6 ($C^{11,11',12,12'}$), 46.1 (C^{10}), 38.1 (C^{20}), 33.4 (C^{18}), 30.9 (C^{15}), 25.7 (C^{14}), 22.9 (C^{19}); R_f 0.39 (DCM : MeOH, 97 : 3, alumina); mp 137–139 °C; *m/z* ($HRMS^+$) 835.3358 ($C_{38}H_{55}O_{11}N_6S_2$ requires 835.3370).

4-[(1-Azathioxanthone)-2-methyl]-10-[2-(methylsulfonylamino)-ethyl]-1,7-bis(α-glutarate)-1,4,7,10-tetraazacyclododecane

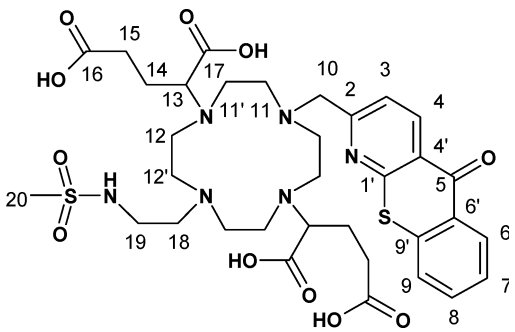

Freshly made KOD solution (2.5 mL, 0.1 M) was added to 4-[(1-azathioxanthone)-2-methyl]-10-[2-(methylsulfonylamino)ethyl]-1,7 - bis(α - dimethylglutarate) - 1,4,7,10 - tetraazacyclododecane (50 mg, 60 μmol). The reaction mixture was kept under argon at room temperature and progress was monitored by NMR. After 3 h no protecting methyl group signals were observed in the ^{1}H-NMR spectrum, the pH of the mixture was increased (pH ≈ 6) with conc. HCl and the solution loaded onto a DOWEX 50 × 4–100 strong cation exchange resin. The column was eluted with water → 10% NH_4OH and the fractions were analysed by $ESMS^+$. The fractions were combined and lyophilised to yield the title compound as a dark orange oil (26 mg, 33 μmol, 55%), which was used for complexation reaction immediately. δ_H ($CDCl_3$) 8.46 (1H, d, *J* 8.0 Hz, H^4), 8.18 (1H, m, H^6), 7.44 (4H, m, $H^{8,9,3,7}$), 3.83 (2H, s, H^{10}), 3.26 (2H, m, H^{13}), 3.02 (3H, s, H^{20}), 3.09 (22H, br m, $H^{11,11',12,12',15,18}$), 2.05 (6H, m, $H^{14,19}$); *m/z* ($ESMS^-$) 779 [M − H].

[H_2EuL^2]

4-[1-(Azathioxanthone)-2-methyl]-10-[2-(methylsulfonylamino)-ethyl] - 1,7 - bis(α - glutarate) - 1,4,7,10 -tetraazacyclododecane (25 mg, 32 μmol) was added to $Eu(CH_3CO_2)_3$ (1.1 eq., 15 mg) and the solids dissolved in H_2O (2 mL). The pH was carefully adjusted to 5 by addition of acetic acid and the reaction left to stir at 70 °C for 72 h. After the reaction was cooled to room temperature, the solvents were removed under reduced pressure and the remaining residue was dissolved in 5 mL H_2O. The pH was then adjusted carefully to 10 by addition of conc. NaOH solution (in order to remove the excess Eu as $Eu(OH)_3$) resulting in a white precipitate, removed *via* a fine syringe filter. The pH was adjusted back to neutral and the mixture lyophilised to give a bright yellow solid (26 mg, 28 μmol). t_R (HPLC) = 10.9 min; *m/z* ($HRMS^-$) 927.1562 ($C_{34}H_{42}O_{11}N_6S_2Eu$ requires 927.1565); $\lambda_{max}(H_2O)$ 380 (4070 $dm^3\ mol^{-1}\ cm^{-1}$); $\tau^{Eu}_{(H2O,\ pH=3.0)}$: 588 ms, $\tau^{Eu}_{(H2O,\ pH=5.5)}$: 709 ms, $\tau^{Eu}_{(H2O,\ pH=8.0)}$: 469 ms; $\tau^{Eu}_{(D2O,\ pD=2.6)}$: 1086 ms, $\tau^{Eu}_{(D2O,\ pD=5.1)}$: 1000 ms, $\tau^{Eu}_{(D2O,\ pD=7.6)}$: 534 ms; $\phi^{Eu}_{(pH=3.0)}$ = 1.8%, $\phi^{Eu}_{(pH=5.5)}$ = 2.0%, $\phi^{Eu}_{(pH=8.0)}$ = 1.7%.

1,7-Bis(α-dimethyladipate)-1,4,7,10-tetraazacyclododecane

Tetraazacyclododecane (1.20 g, 6.98 mmol), dimethyl 2-bromoadipate (3.88 g, 15.35 mmol) was dissolved in dry MeCN (20 mL) followed by addition of $NaHCO_3$ (1.29 g, 2.2 eq.). The mixture was stirred at 55 °C under argon. The reaction was monitored by TLC (DCM : THF : MeOH, 50 : 50 : 5) and $ESMS^+$. After 4 days of reaction all dimethyl 2-bromoadipate had been consumed, and the solvent was removed under reduced pressure. The remaining residue was dissolved in DCM (10 mL). The organic layer was washed with HCl (pH 3), dried over K_2CO_3 and the solvents removed under reduced pressure. The residue was purified by column chromatography over silica (DCM : THF : MeOH, 50 : 50 : 3). The fractions containing the title product were combined and the solvents were removed under reduced pressure to yield a transparent viscous oil which slowly crystallised to reveal a white solid (760 mg, 1.47 mmol, 21%). δ_H ($CDCl_3$) 4.18 (1H, m, H^3) 3.77 (6H, s, H^7), 3.73 (6H, s, H^8), 3.29 (16H, m, $H^{1,2}$), 2.36 (4H, m, H^6), 1.78 (8H, m, $H^{4,5}$); δ_C ($CDCl_3$) 174.0 ($C^{7'}$), 173.9 ($C^{8'}$), 70.3 (C^3), 53.0 (C^8), 52.7 (C^7), 52.6, 52.1, 51.8, 46.6 ($C^{1,2}$), 33.7 (C^4), 33.6 (C^6), 31.0 (C^5); *m/z* ($ESMS^+$) 517 [M + H], 530 [M + Na]; R_f 0.42 (THF : DCM : MeOH, 50 : 50 : 5, silica).

4-[(1-Azathioxanthone)-2-methyl]-1,7-bis(α-dimethyladipate)-1,4,7,10-tetraazacyclododecane

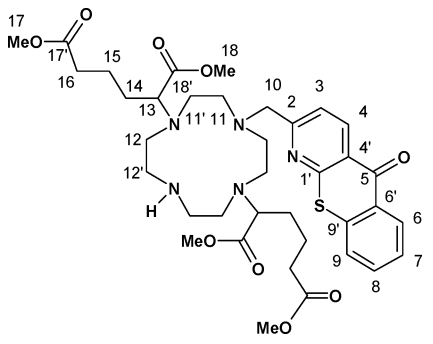

1,7 - Bis(α - dimethyladipate) - 1,4,7,10 - tetraazacyclododecane (310 mg, 600 μmol) was combined with 2-bromomethyl-1-azathiaxanthone (1 eq., 183 mg) and $NaHCO_3$ (1 eq., 50 mg) and the mixture stirred in dry MeCN (10 mL), was heated initially at 60 °C for 4 h followed by 70 °C for 20 h under argon. The reaction was monitored by TLC (DCM : THF : MeOH :

Et_3N, 80 : 20 : 3.5 : 3.5, silica) and $ESMS^+$ to confirm that the brominated starting material had been consumed. The solvent was removed under reduced pressure and the resulting solid was dissolved in a small volume of DCM (5 mL) and the sodium salts removed by filtration. The crude mixture was purified by column chromatography (DCM : THF 80 : 20 → 3% MeOH : Et_3N (1 : 1)); fractions containing clean product were combined and the solvents were removed under reduced pressure. The remaining residue was dissolved in DCM (5 mL) and washed with water (3 × 15 mL). The organic layer was evaporated dry to yield the title compound as a pale yellow oil (165 mg, 170 μmol, 28%). δ_H ($CDCl_3$) 8.80 (1H, d, *J* 8.0 Hz, H^4), 8.60 (1H, br d, *J* 7.9 Hz, H^6), 7.67 (2H, m, $H^{8,9}$), 7.55 (1H, dt, *J* 7.9 Hz, H^7), 7,34 (1H, d, *J* 8.0 Hz, H^3), 4.19 (1H, m, H^{13}), 3.81 (2H, s, H^{10}), 3.73 (6H, s, H^{17}), 3.69 (6H, s, H^{18}), 3.17 (16H, m, $H^{11,11',12,12'}$), 2.38 (4H, m, H^{16}), 1.78 (8H, m, $H^{14,15}$); δ_C ($CDCl_3$) 181.2 (C^5) 173.4 ($C^{16'}$), 172.9 ($C^{17'}$), 162.1 (C^2), 158.8 ($C^{1'}$), 138.4 ($C^{4'}$), 137.5 ($C^{6'}$), 133.4 (C^8), 130.2 (C^6), 129.1 ($C^{9'}$), 127.1 (C^7), 126.7 (C^9), 125.8 (C^4), 122.5 (C^3), 70.3 (C^{13}), 52.0 (C^{18}), 51.8 (C^{17}), 51.9, 51.8, 51.7, 49.2 ($C^{11,11',12,12'}$), 48.1 (C^{10}), 33.8 (C^{14}), 33.7 (C^{16}), 29.9 (C^{15}); R_f 0.33 (DCM : THF : MeOH : Et_3N, 80 : 20 : 3.5 : 3.5, silica plate); *m/z* ($HRMS^+$) 742.3489 ($C_{37}H_{52}O_9N_5S$ requires 742.3486).

4-[(1-Azathioxanthone)-2-methyl]-10-[2-(methylsulfonylamino)-ethyl]-1,7-bis(α-dimethyladipate)-1,4,7,10-tetraazacyclododecane

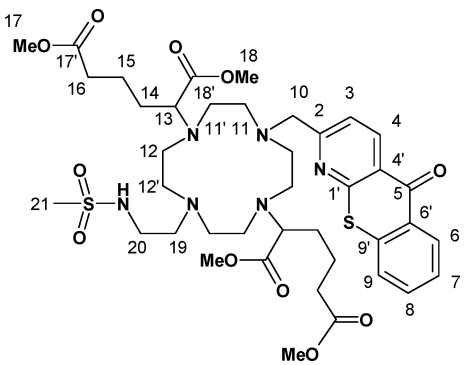

4-[(1-Azathioxanthone)-2-methyl]-1,7-bis(α-dimethyladipate)-1,4,7,10-tetraazacyclododecane (190 mg, 256 μmol) was combined with 2-methanesulfonato-*N*-methanesulfonylethylamine (1.2 eq., 67.2 mg) and Na_2CO_3 (1.5 eq., 42 mg) and the mixture stirred in dry MeCN (10 mL) at reflux for 30 h under argon. The reaction was monitored by TLC (DCM : THF : MeOH : Et_3N, 80 : 20 : 2.5 : 2.5, silica) and $ESMS^+$ to confirm that the starting material had been consumed. The solvent was removed under reduced pressure. The resulting solid was dissolved in a small volume of DCM (5 mL) and the sodium salts were filtered out. The crude mixture was purified by column chromatography (DCM : THF 80 : 20 → 3% MeOH : Et_3N (1 : 1)). The fractions containing product only were combined and the solvents were removed under reduced pressure. The remaining residue was dissolved in DCM (5 mL) and washed with water (3 × 10 mL). The organic layer was evaporated to yield the title compound as a pale brown oil (170 mg, 197 μmol, 77%). δ_H ($CDCl_3$) 8.80 (1H, d, *J* 8.0 Hz, H^4), 8.66 (1H, br d, *J* 7.9 Hz, H^6), 7.76 (2H, dd, *J* 7.9 Hz, $H^{8,9}$), 7.65 (1H, dt, *J* 7.9 Hz, H^7), 7.53 (1H, d, *J* 8.0 Hz, H^3), 4.19 (1H, m, H^{13}), 3.84 (2H, s, H^{10}), 3.66 (6H, s, H^{17}), 3.64 (6H, s, H^{18}), 3.06 (16H, m, $H^{11,11',12,12'}$), 2.98 (3H, dd, H^{21}), 2.33 (6H, m, $H^{16,19}$), 1.68 (10H, m, $H^{14,15,20}$); δ_C ($CDCl_3$) 180.8 (C^5) 174.9 ($C^{18'}$), 173.5 ($C^{17'}$), 165.4 (C^2), 158.1 ($C^{1'}$), 138.1 ($C^{4'}$), 137.7 ($C^{6'}$), 133.1 (C^8), 130.1 (C^6), 129.2 ($C^{9'}$), 126.9 (C^7), 126.7 (C^9), 125.8 (C^4), 121.7 (C^3), 65.7 (C^{13}), 51.8 (C^{18}), 51.4 (C^{17}), 54.3, 54.1, 50.2, 50.1 ($C^{11,11',12,12'}$), 50.0 (C^{10}), 40.1 (C^{21}), 34.4 (C^{14}), 33.8 (C^{16}), 30.6 (C^{19}) 29.6 (C^{15}), 22.3 (C^{20}); R_f 0.61 (DCM : THF : MeOH : Et_3N, 80 : 20 : 2.5 : 2.5, silica); *m/z* ($HRESMS^+$) 863.3686 ($C_{40}H_{58}O_{11}N_6S_2$ requires 863.3679).

4-[(1-Azathioxanthone)-2-methyl]-10-[2-(methylsulfonylamino)-ethyl]-1,7-bis(α-adipate)-1,4,7,10-tetraazacyclododecane, H_5L_3

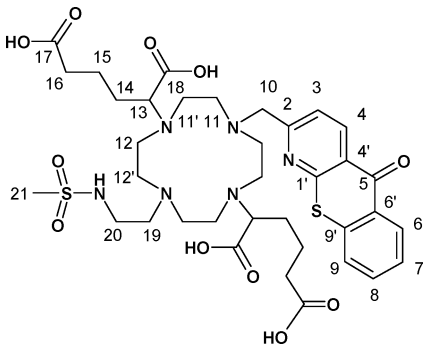

Freshly made KOD solution (5 mL, 0.1 M) was added to 4-[(1-azathioxanthone)-2-methyl]-10-[2-(methylsulfonylamino)ethyl]-1,7 - bis(α - dimethyladipate) - 1,4,7,10 - tetraazacyclododecane (57 mg, 66 μmol) and the mixture was stirred under argon at room temperature; the reaction was monitored by ^1H-NMR. After 3 h no methyl group signals were observed in the ^1H-NMR spectrum; the pH of the mixture was adjusted (pH ≈ 6) with conc. HCl, washed with DCM (3 × 5 mL) and loaded onto a DOWEX 50 × 4–100 strong cation exchange resin. The column was eluted with water → 10% NH_4OH and the fractions were analysed by $ESMS^+$. The appropriate fractions were combined and lyophilised to yield the title compound as a dark orange oil (25 mg, 33 μmol, 47%), which was used in a complexation reaction immediately. δ_H ($CDCl_3$) 8.55 (1H, d, *J* 8.0 Hz, H^4), 8.24 (1H, m, H^6), 7.49 (4H, m, $H^{8,9,3,7}$), 3.16 (27H, br m, $H^{10,11,11',12,12',16,19,21}$), 1.67 (10H, m, $H^{14,15,20}$); *m/z* ($ESMS^-$) 805 [M − H].

[H_3EuL^3]

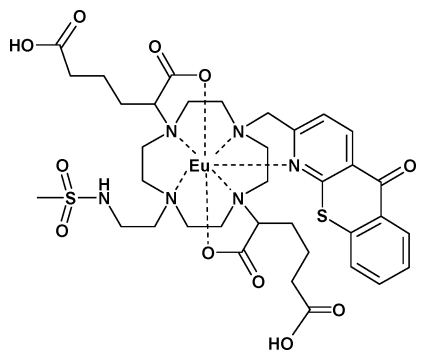

4-[(1-Azathioxanthone)-2-methyl]-10-[2-(methylsulfonylamino)-ethyl]-1,7-bis(α-adipate)-1,4,7,10-tetraazacyclododecane (25 mg, 31 μmol) was added to $Eu(OAc)_3$ (1.1 eq., 13 mg) and the solids

dissolved in 2.5 mL H_2O : MeOH (5 : 1). The pH was carefully adjusted to 5 by addition of acetic acid and the reaction left to stir at 75 °C for 72 h. After the reaction was cooled to room temperature, the pH was then adjusted carefully to 10 by addition of conc. NaOH solution (in order to remove excess Eu as $Eu(OH)_3$) resulting in a white precipitate removed *via* centrifugation. The pH was adjusted back to neutral and the sample lyophilised to give a bright yellow solid (30 mg, 30 μmol). t_R (HPLC) = 11.2 min; *m/z* (HRMS$^+$) 979.1846 ($C_{36}H_{47}O_{11}N_6S_2EuNa$ requires 979.1849); $\lambda_{max}(H_2O)$ 380 (4070 $dm^3\ mol^{-1}\ cm^{-1}$); $\tau^{Eu}_{(H2O,\ pH=4.5)}$: 830 ms, $\tau^{Eu}_{(H2O,\ pH=8.0)}$: 430 ms; $\tau^{Eu}_{(D2O,\ pD=4.1)}$: 825 ms, $\tau^{Eu}_{(D2O,\ pD=7.6)}$: 470 ms; $\phi^{Eu}_{(pH=4.5)} = 6.1\%$, $\phi^{Eu}_{(pH=8.0)} = 5.3\%$.

[H_3GdL^3]

The Gd-complex was prepared as described above for [H_3EuL^3], t_R (HPLC) = 11.5 min; *m/z* (HRMS$^-$ in MeOH) 1001.2299 ($C_{36}H_{49}O_{11}N_6S_2GdNa$ mono Me-ester requires: 1001.2273); $r_{1p}{}^{(pH=4.5)}$: 3.12 $mM^{-1}\ s^{-1}$ $r_{1p}{}^{(pH=8.5)}$: 1.87 $mM^{-1}\ s^{-1}$.

Acknowledgements

We thank the EC networks of excellence, EMIL (503659) and DIMI (512146). Elizabeth New for the toxicity assay work and the Royal Society for support.

References

1 (*a*) R. A. Gatenby, R. J. Gillies, E. T. Gawlinski, A. F. Gmitro and B. Kaylor, *Cancer Res.*, 2006, **66**, 5216; (*b*) R. J. Gillies, N. Raghunand, M. L. Garcia-Martin and R. A. Gatenby, *I/EEE Engineering in Medicine and Biology Magazine*, 2004, **23**, 57.
2 Y. Song, D. Salinas, D. W. Nielson and A. S. Verkman, *Am. J. Physiol.: Cell Physiol.*, 2006, **290**, 741.
3 F. L. M. Ricciardolo, B. Gatston, J. Hunt and J. Allergy, *Clin. Immunol. (San Diego, CA, U. S.)*, 2004, **113**, 610.
4 G. Helmlinger, F. Yuan, M. Dellian and R. K. Jain, *Nat. Med.*, 1997, **3**, 177.
5 O. V. Vieira, R. J. Bothelo and S. Grinstein, *Biochem. J.*, 2002, **366**, 689.
6 R. Weissleder and V. Ntziachritos, *Nat. Med.*, 2003, **9**, 123.
7 M. E. Cooper, S. Gegory, E. Aidie and S. Kalinka, *J. Fluoresc.*, 2002, **12**, 425.
8 P. T. Snee, R. C. Somers, G. Nair, J. P. Zimmer, M. G. Bawendi and D. G. Nocera, *J. Am. Chem. Soc.*, 2006, **128**, 13320.
9 L. Sterowski, J. C. Mason, H. Lee, M. Say and G. Patonay, *J. Heterocycl. Chem.*, 2004, **41**, 227.
10 Z. Zhang and S. Achilefu, *Chem. Commun.*, 2005, 5887.
11 T. J. Rink, R. Y. Tsien and T. Pozzan, *J. Cell Biol.*, 1982, **95**, 189.
12 R. Weissleder and S. A. Hildebrand, *Chem. Commun.*, 2007, 2747.
13 G. Grynkiewicz, M. Poenie and R. Y. Tsien, *J. Biol. Chem.*, 1985, **260**, 3440; O. S. Wolfbeis, *J. Mater. Chem.*, 2005, **15**, 2657.
14 T. Gunnlaugsson and J. P. Leonard, *Chem. Commun.*, 2005, 3114; D. Parker, J. A. G. Williams and P. K. Senanayake, *J. Chem. Soc., Perkin Trans. 2*, 1998, 2129; C. P. McCoy, F. Stomeo, S. E. Plush and T. Gunnlaugsson, *Chem. Mater.*, 2006, **18**, 4336; D. Parker and J. A. G. Williams, *Chem. Commun.*, 1998, 245; T. Gunnlaugsson and D. Parker, *Chem. Commun.*, 1998, 511; A. P. de Silva, H. Q. N. Gunaratne and T. E. Rice, *Angew. Chem., Int. Ed. Engl.*, 1996, **35**, 2116; C. Baxicaluppi, A. Bencini, A. Bianchi, A. Giorgi, V. Fusi, A. Masotti, B. Valtancoli, A. Roque and F. Pina, *Chem. Commun.*, 2000, 561.
15 (*a*) For examples immobilised in sol gel or hydrogel matrices: S. Blair, M. P. Lowe, C. E. Mathieu, D. Parker, P. K. Senanayake and R. Kataky, *Inorg. Chem.*, 2001, **40**, 5860; C. P. McCoy, F. Stomeo, S. E. Plush and T. Gunnlaugsson, *Chem. Mater.*, 2006, **18**, 4336; (*b*) M. Woods and A. D. Sherry, *Inorg. Chem.*, 2003, **42**, 4401; (*c*) For some reviews, see: D. Parker, S. Pandya and J. Yu, *Dalton Trans.*, 2006, 2757; D. Parker, *Coord. Chem. Rev.*, 2000, **205**, 109.
16 (*a*) M. P. Lowe, D. Parker, O. Reany, S. Aime, M. Botta, G. Castellano, E. Gianolio and R. Pagliarin, *J. Am. Chem. Soc.*, 2001, **123**, 7601; M. P. Lowe and D. Parker, *Chem. Commun.*, 2000, 707; (*b*) Y. Bretonniere, M. J. Cann, D. Parker and R. J. Slater, *Org. Biomol. Chem.*, 2004, **2**, 1624; Y. Bretonniere, M. J. Cann, D. Parker and R. J. Slater, *Chem. Commun.*, 2002, 1930.
17 (*a*) R. S. Dickins, D. Parker, J. I. Bruce and D. J. Tozer, *Dalton Trans.*, 2003, 1264; D. Parker, *Chem. Soc. Rev.*, 2004, **33**, 156; (*b*) For earlier empirical studies, see O. L. Malta, H. J. Batista and L. D. Carlos, *Chem. Phys.*, 2002, **282**, 21; (*c*) R. Pal and D. Parker, *Chem. Commun.*, 2007, 474.
18 S. Quici, G. Marzanni, M. Cavazipni, P. L. Anelli, M. Botta, E. Gianolio, G. Accorsi, N. Armaroli and F. Barigelletti, *Inorg. Chem.*, 2002, **41**, 2777; G. Bobba, J. C. Frias and D. Parker, *Chem. Commun.*, 2002, 890.
19 (*a*) R. A. Poole, F. Kielar, S. L. Richardson, P. A. Stenson and D. Parker, *Chem. Commun.*, 2006, 4084; (*b*) D. Parker and J. Yu, *Chem. Commun.*, 2005, 3141.
20 P. Atkinson, K. S. Findlay, F. Kielar, R. Pal, D. Parker, R. A. Poole, H. Puschmann, S. L. Richardson, P. A. Stenson, A. L. Thompson and J. Yu, *Org. Biomol. Chem.*, 2006, **4**, 1707.
21 (*a*) R. S. Dickins, D. Parker, A. S. de Sousa and J. A. G. Williams, *Chem. Commun.*, 1996, 697; (*b*) A. Beeby, I. M. Clarkson, R. S. Dickins, S. Faulkner, L. Royle, D. Parker, A. S. de Sousa, J. A. G. Williams and M. Woods, *J. Chem. Soc., Perkin Trans. 2*, 1999, 493.
22 P. Caravan, *Chem. Soc. Rev.*, 2006, **35**, 512; S. Aime, A. S. Batsanov, M. Botta, J. A. K. Howard, D. Parker, P. K. Senanayake and J. A. G. Williams, *Inorg. Chem.*, 1994, **33**, 4696; O. Bottrill, L. Kwok and N. J. Long, *Chem. Soc. Rev.*, 2006, **35**, 557.
23 J. Yu, R. Pal, D. Parker, R. A. Poole and M. J. Cann, *J. Am. Chem. Soc.*, 2006, **128**, 2294.
24 J. Ghuman, P. A. Zunszain, I. Peptitpas, A. A. Bhattacharya, M. Otagiri and S. Curry, *J. Mol. Biol.*, 2005, **353**, 38.
25 J. Stevens, *J. Cell Biol.*, 1965, **24**, 349.
26 M. Horky, V. Kotala, M. Anton and J. Wesierska-Gadek, *Ann. N. Y. Acad. Sci.*, 2002, **973**, 258.
27 J. Carmichael, W. G. DeGraff, A. F. Gazdar, J. D. Minna and J. B. Mitchell, *Cancer Res.*, 1987, **47**, 936–942.
28 L. Pentz and E. R. Thornton, *J. Am. Chem. Soc.*, 1967, **89**, 6931.
29 A. K. Covington, M. Paabo, R. A. Robinson and R. G. Bates, *Anal. Chem.*, 1960, **40**, 700.